Optics Communications 381 (2016) 286–291

Contents lists available at ScienceDirect

Optics Communications

journal homepage: www.elsevier.com/locate/optcom

Optical biosensor based on liquid crystal droplets for detection of cholic acid

Xiaofang Niu [a], Dan Luo [a,*], Rui Chen [a], Fei Wang [a], Xiaowei Sun [a], Haitao Dai [b]

[a] Department of Electrical & Electronic Engineering, Southern University of Science and Technology, Xueyuan Road 1088, Nanshan District, Shenzhen, Guangdong 518055, China

[b] Tianjin Key Laboratory of Low Dimensional Materials Physics and Preparing Technology, School of Science, Tianjin University, Weijin Road 92, Nankai, Tianjin 300072, China

ARTICLE INFO

Article history:
Received 12 April 2016
Received in revised form
1 July 2016
Accepted 6 July 2016
Available online 22 July 2016

Keywords:
Optical biosensor
Liquid crystal
Cholic acid

ABSTRACT

A highly sensitive cholic acid biosensor based on 4-cyano-4′-penthlbiphenyl (5CB) Liquid crystal droplets in phosphate buffer saline solution was reported. A radial-to-bipolar transition of 5CB droplet would be triggered during competitive reaction of CA at the sodium dodecyl sulfate surfactant-laden 5CB droplet surface. Our liquid crystal droplet sensor is a low-cost, simple and fast method for CA detection. The detection limit (5 μM) of our method is 2.4 times lower than previously report by using liquid crystal film to detection of CA.

1. Introduction

Bile acids (mainly contain cholic, deoxycholic, and lithocholic acid) are important steroidal compounds, which are produced in the liver from cholesterol and play a significant physiological role in digestion and absorption of dietary lipids and fat-soluble vitamins through emulsification [1,2]. In addition, cholic acid (CA) is one of primary bile acids as it weighs more than 31% in all of bile acid and the concentration of CA is connected with liver cancer (hepatocellular carcinoma), gallstone and other diseases [3,4]. The concentration of CA is normally in range of 1–5 mM in liver and less than 10 μM in human's serum [5,6]. For these reasons, developing a strategy to detect the concentration level of CA is particularly critical.

In recent years, many methods have been developed for the detection of CA. For example, thin-layer chromatography [7], gas chromatography (GC) [8], supercritical fluid chromatography (SFC) [9], optical spectrum analyzer [10], molecularly imprinted [11], high-performance liquid chromatography (HPLC) and mass spectrometry (MS) [12–14]. However, these methods require expensive instruments and complex operational processes. Low-cost, simple and fast analytical method for cholic acid is highly desirable.

With the development of optical device, more and more optical methods have attracted attentions because of their potential utility with specific, direct detection process, low cost and less time consuming of analysis, compared to conventional assay techniques. Among them, liquid crystal (LC) is a promising candidate of optical biological sensor due to their unique properties of large birefringence and high sensitivity of the orientations of liquid crystal molecules to tiny variation on the surface [15,16]. Molecule events occurred at an LC/aqueous interface can be amplified and transduced through orientation changes of LC molecules into optical signals, which are visible by the naked eye under polarizing optical microscope [17,18].

LC droplets have been widely used in environmental and biomedical science as a sensor with high sensitivity [19,20]. Several research groups have utilized LC droplets for the detection of viruses, bacteria, avidin, cancer cells and protein [21–24]. Merola et al. maneuvered fragmental nematic LC on the substrate surface and achieved different configurations LC droplets in electric field, which can be used as spatial modulation [25]. Hu et al. demonstrated a sensing device, which used to examined water vapors, amphiphiles, and vapors of volatile organic compound (VOCs), where the LC was dissolved in organic solvents on glass microscope slides and distinctive optical textures that represent different orientations of LCs was observed under a polarizing optical microscope [26]. He et al. reported a sensor based on LC layer for detection CA [27]. However, the multilayer of LC leads to a strong anchoring force, which is not easy to be disturbed by CA thus the sensitivity can be furthur improved.

* Corresponding author. Present address: Department of Electrical & Electronic Engineering, South University of Science and Technology of China, China.
E-mail address: luo.d@sustc.edu.cn (D. Luo).

http://dx.doi.org/10.1016/j.optcom.2016.07.016
0030-4018/

Herein we proposed a low-cost, simple and fast method for CA detection based on LC droplets. Sodium dodecyl sulfate (SDS) was coated on the surface of 4-cyano-4′-penthlbiphenyl (5CB) liquid crystal droplets, which resulted to a radial configuration of LC droplets in phosphate buffer saline (PBS) solution. A radial-to-bipolar transition of 5CB droplet will be triggered during competitive reaction of CA at the SDS surfactant-laden 5CB droplet surface when certain amount, beyond detection limit, of CA was added. The detection limit (5 μM) of our method is 2.4 times lower than previously report by using liquid crystal film to detection of CA.

2. Materials and methods

2.1. Chemicals and materials

Sodium chloride (NaCl), sodium dodecyl sulfate (SDS, > 98%), sodium hydroxide (NaOH), phosphate buffer saline (PBS) (10 mM phosphate, 138 mM NaCl, 2.7 mM KCl; pH 7.4), and cholic acid (CA) were all purchased from Sigma-Aldrich. 4-n-pentyl-4′-cyanobiphenyl (5CB) was bought from HCCH (Jiangsu Hecheng, China). Microscope slides (25.4 mm × 76.2 mm, 1 mm thick) were purchased from Sail Brand (Shanghai, China). Glass cover slides (Sail Brand) were obtained from Taizhou Dongsheng Glass Co. Ltd., China. All aqueous solutions were prepared using double-deionized water obtained from a Millipore Ultra-Pure Reagent Water System (Millipore, Continental Water Systems, ElPaso, TX, USA). All experiments were carried out at 25 °C.

2.2. Preparation and observation of liquid crystal droplets

Microscope glass slide was cleaned using a hot piranha solution (H_2SO_4 (98%): H_2O_2 (35%) = 3:1) for 30 min (caution: piranha solution is extremely corrosive and must be handled carefully). Then it was washed with deionized water and dried under nitrogen. Acrylic ab adhesive was used as rampart paint on the functionalized glass slide. Optical images of LC droplets were observed using polarizing optical microscope (Ti 200, Nikon) in transmission mode.

3. Results and discussions

3.1. Fabrication of LC cell

A LC cell with thickness of 200 μm and size of 10 × 10 mm was assembled by a glass side and a coverslip, sealed by acrylic AB adhesive as in Fig. 1(a). Sodium dodecyl sulfate (SDS) is a kind of surfactant, coated by oleophilic long alkyl chain and hydrophilic chemical group. When LC droplets contacted with SDS in the PBS solution, the SDS will adhere to the surface of LC droplets due to their oleophilic long alkylchain, leading to the formation of SDS-laden 5CB droplet/aqueous surface. This reaction is illustrated in Fig. 1(b). Due to good hydrophobicity of 5CB, a nematic liquid crystal (5CB here) droplet naturally acquires a spherical shape with an internal radial director configuration when dispersed in SDS. The polarizing optical microscope image showed typical cross dark lines in droplets, as shown in Fig. 1(c).

When CA is added into the solution containing 5CB droplets with SDS-Laden surface, a radial to bipolar configuration would be triggered. The reason is that the CA prefers to adsorb at the surface of LC molecule through the interface competitive adsorption with the SDS-laden 5CB droplet/aqueous, which leaded to a change in LC droplets and became bipolar configuration. The schematic and polarizing optical microscope image of bipolar configuration is shown in Fig. 1(d), where a dark line is observed in bipolar configuration.

3.2. Preparation of LC droplets

According to Oscar's report, droplets should fragmentate from a large size to small in a criticality condition [28]. In forming process of LC droplets, the size of LC droplets depends on the stirring time in mixing. Fig. 2(a)–(e) shows polarization optical microscopy images of 5CB droplets with different stirring time of 6 s, 60 s, 120 s, 180 s, and 240 s, where the stirring speed is 600 rpm and the volume ratio of LC and SDS is 1:15. Fig. 2(f) shows the different diameters obtained under different stirring time. The size of LC droplets decreases with the increase of stirring times increased. After mixing, the mixture was injected into the LC cell with 10 mM of PBS.

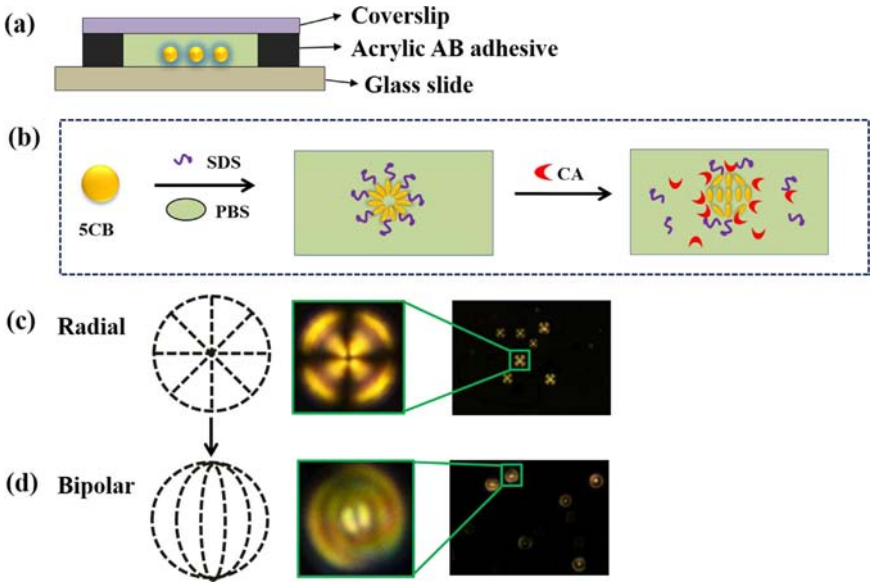

Fig. 1. (a) Liquid crystal cell structure; (b) schematic illustration of the competition absorption of CA at the SDS-laden 5CB droplet/aqueous surface; (c) radial configuration and corresponding polarization optical microscopy image of 5CB droplets without CA in PBS solution; (d) bipolar configuration and polarization optical microscopy image of 5CB droplets with CA in PBS solution.

Please cite this article as: X. Niu, et al., Optics Communications (2016), http://dx.doi.org/10.1016/j.optcom.2016.07.016

As the surfactant of SDS could adsorb the 5CB molecule (with a strong hydrophobic property), the LC droplets is in a radial configuration under the polarizing optical microscope. Fig. 3 shows the optical images of 5CB droplets added with different amount of SDS. When the concentration of SDS was less than 50 μM, no typical cross dark line corresponding to radial configuration was observed. Fig. 3(a) and (b) show the optical images of 5CB droplets with SDS's concentration of 5 μM and 20 μM. When 50 μM SDS was added, a typical radial configuration of LC droplets was observed in polarization optical microscopy, as shown in Fig. 3(c), indicating the threshold of SDS concentration for forming 5CB droplets with radial configuration is 50 μM.

3.3. Optimal experimental condition for detection of CA

In order to identify the transform time of LC droplets by CA, further study was conducted in the detection process. The verification test was required and shown in Fig. 4. It can be seen that the LC droplet shows a cross image in polarizing optical microscope in Fig. 4(a). However, once CA was added to the system, the cross transformed quickly and turn into a ring after 40 s and the state almost remained stable after CA was added more than 50 s. Therefore, 50 s was selected as the optimal reaction time.

Because the pH value influenced the configuration of LC droplets, we also investigated the effect of pH on 5CB droplets configuration. In our experiment, the SDS solution was prepared in different pH value varying from 4 to 8 while keeping the adding amount of CA unchanged to be 1 mM in the solution. We can see that LC droplets shown an incomplete circle and irregular blue center when the pH was 4 in Fig. 5(a). When the pH was 5, the LC droplet appeared less incomplete circle and the irregular center showed a bright color in Fig. 5(b). When the pH increased to 6, the LC droplets became a perfect ball and shown two pole on the surface of the droplets in Fig. 5(c). It suggest that 5CB formed a bipolar configuration in the droplets. However, after the pH value was far from 6, the LC droplets shown a concentric ring without two pole, such as pH=7 in Fig. 5(d). In this condition, 5CB have not shown a bipolar configuration in the droplets. The reason possibly is that phase change of 5CB in the system. Based on above results, we can see that the pH of 6 was the best experimental condition, which leads to a perfect bipolar configuration of 5CB droplets.

When CA was added to 5CB with SDS solution, a configuration transition of 5CB droplets was triggered, which was a result of the competitive adsorption of CA at the surface. Fig. 6 shows the obtained polarizing optical microscope images when different concentration of CA was added into the SDS-laden 5CB droplets/aqueous surface, where pH=6. The corresponding optical images of 5CB droplets gradually changed from radial configuration to bipolar configuration with increasing CA concentration. When CA concentration was lower than 5 μM in Fig. 6(a), the configuration transition was not triggered and optical image of LC droplets kept unchanged with radial configuration. When the concentration of

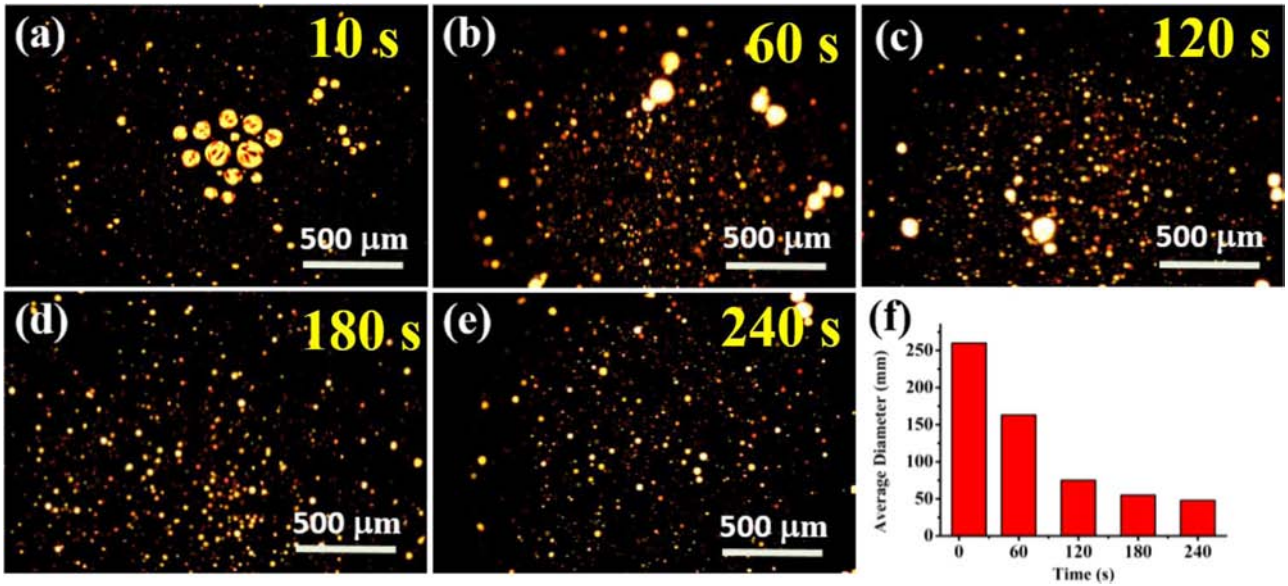

Fig. 2. Polarization optical microscopy images of 5CB droplets with different stirring time (a) 6 s; (b) 60 s; (c) 120 s; (d) 180 s; (e) 240 s; (f) relationship of average diameter of droplets formed with stirring time. Scale bar: 500 μm.

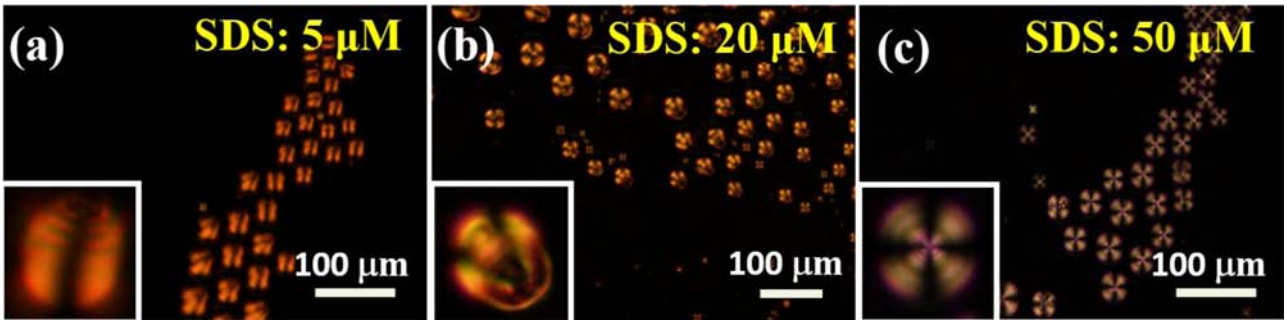

Fig. 3. Polarization optical microscopy images of 5CB droplets. The SDS concentration is (a) 5 μM, (b) 20 μM, and (c) 50 μM, respectively. Scale bar: 100 μm.

Please cite this article as: X. Niu, et al., Optics Communications (2016), http://dx.doi.org/10.1016/j.optcom.2016.07.016

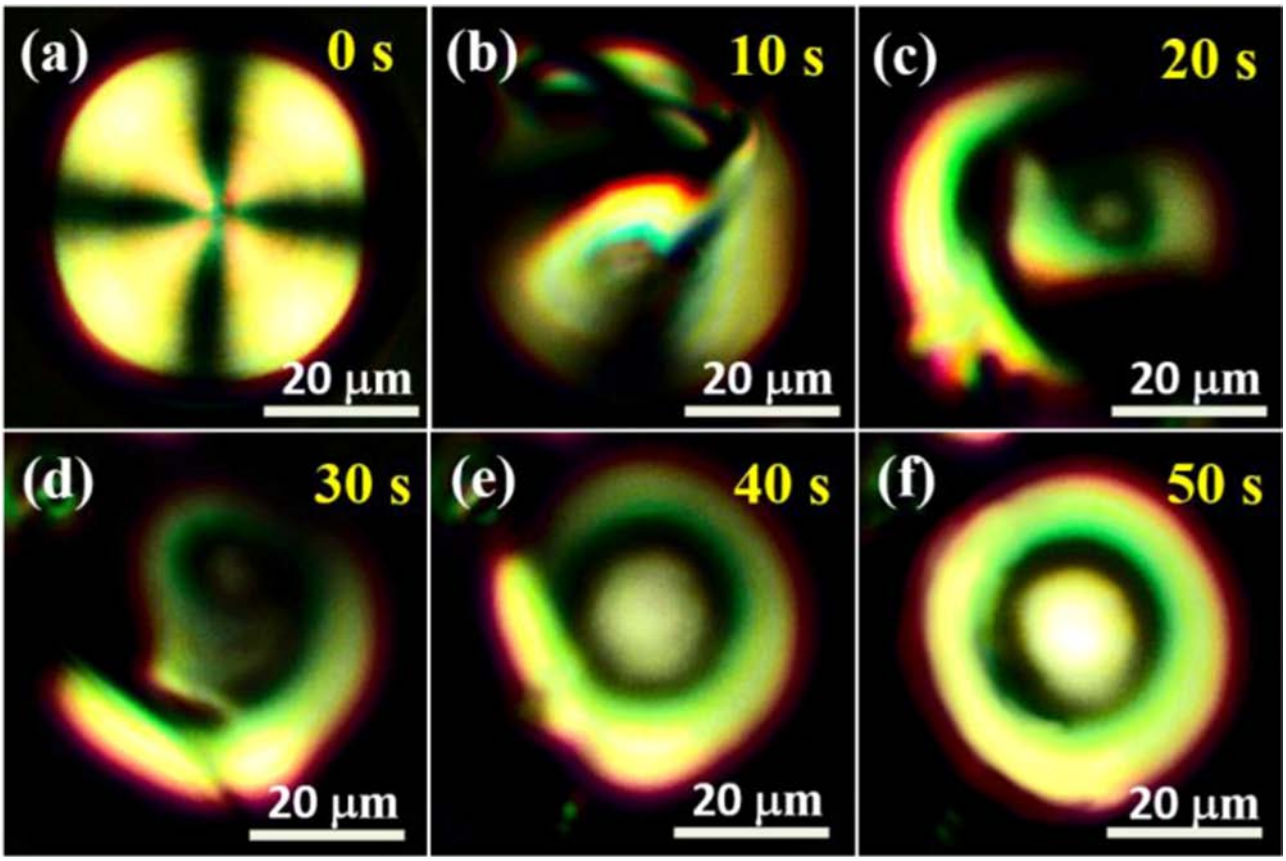

Fig. 4. The transform of LC droplet induced by CA in polarizing optical microscope. (a) Before CA was added to the LC droplet. From (b)–(f), the transform time was 10 s, 20 s, 30 s, 40 s, and 50 s.

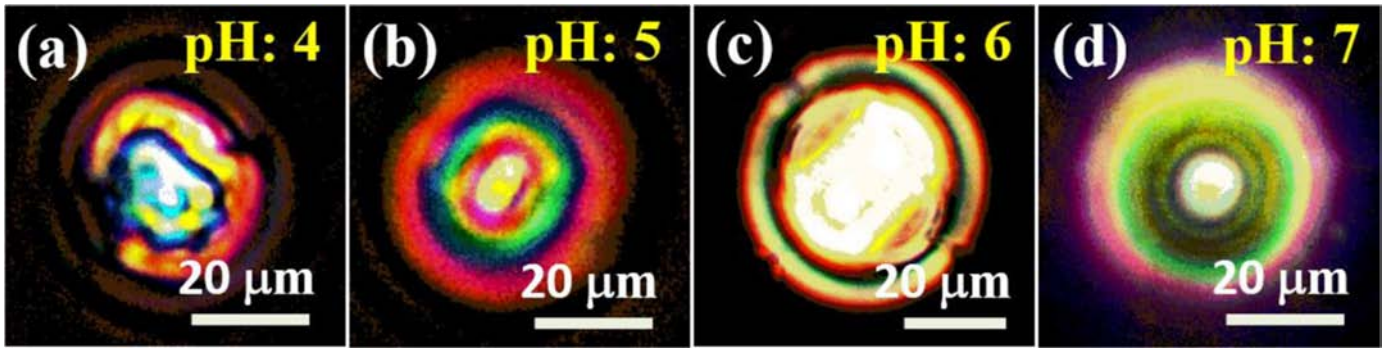

Fig. 5. The optical images of LC droplet at different pH: (a) pH=4; (b) pH=5; (c) pH=6; and (d) pH=7.

CA reached 5 μM, a radial-to-bipolar transition of 5CB droplet was triggered and the optical image of LC droplets started to change from radial to bipolar configuration was shown in Fig. 6(b). It have two states of radial and bipolar configuration and the detection limit for CA was 5 μM. With increase the concentration of CA, more and more droplets shown bipolar configuration in Fig. 6 (c) and (d).

3.4. The selectivity of LC biosensor

In human body, lithocholic acid (LCA) and CA take a large percentage in bile acid. Therefore, it is important to study the interference of LCA on LC droplets. In our experiment, 1 mM of PBS, 1 mM of LCA, and 300 μM of CA were tested under the same condition. The corresponding polarization optical images are shown in Fig. 6(a)–(c). We can see that LC droplets maintain typical radial configuration when 1 mM PBS is added into the 5CB with SDS solution in Fig. 7(a), indicating that the PBS cannot replace the SDS on the surface of 5CB droplets. In Fig. 7(b), the LC droplets exhibit a tiny different when the LCA was added, which suggests that the LCA only have no significant effect on this biosensor. The underlying reason might be that the structure of LCA, which have no hydroxyl on the 12-position, thus leads to no significant competition with SDS. However, in contrast, a radial-to-bipolar transition has been observed in the polarizing optical microscope when 300 μM of CA is added, as shown in Fig. 7(c). All of above results indicate that the PBS and LCA have negligible response of 5CB droplets with SDS, and this type of LC droplet sensor is particular sensitive to CA.

Because the surfactant plays a key role in configuration transition of 5CB droplet, several kinds of surfactants were used in 5CB to detect CA. From Fig. 7(d), we can see that, the detection limits of etraethylene glycol monododecyl ether ($C_{12}E_4$), hexadecyl trimethyl ammonium Bromide (CTAB), dodecyl trimethyl ammonium

Please cite this article as: X. Niu, et al., Optics Communications (2016), http://dx.doi.org/10.1016/j.optcom.2016.07.016

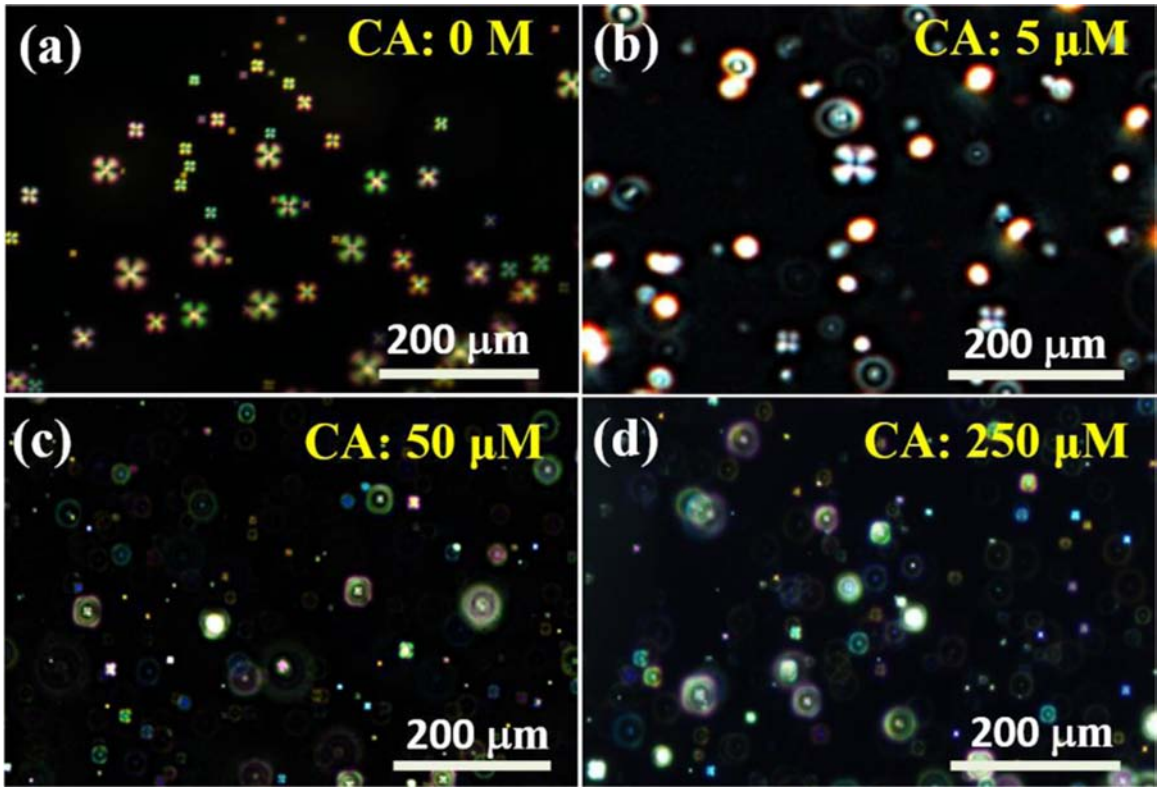

Fig. 6. LC droplets detection of CA at different concentrations. (a): 0 M; (b): 5 μM; (c): 25 μM; and (d): 50 μM. Scale bar: 200 μm.

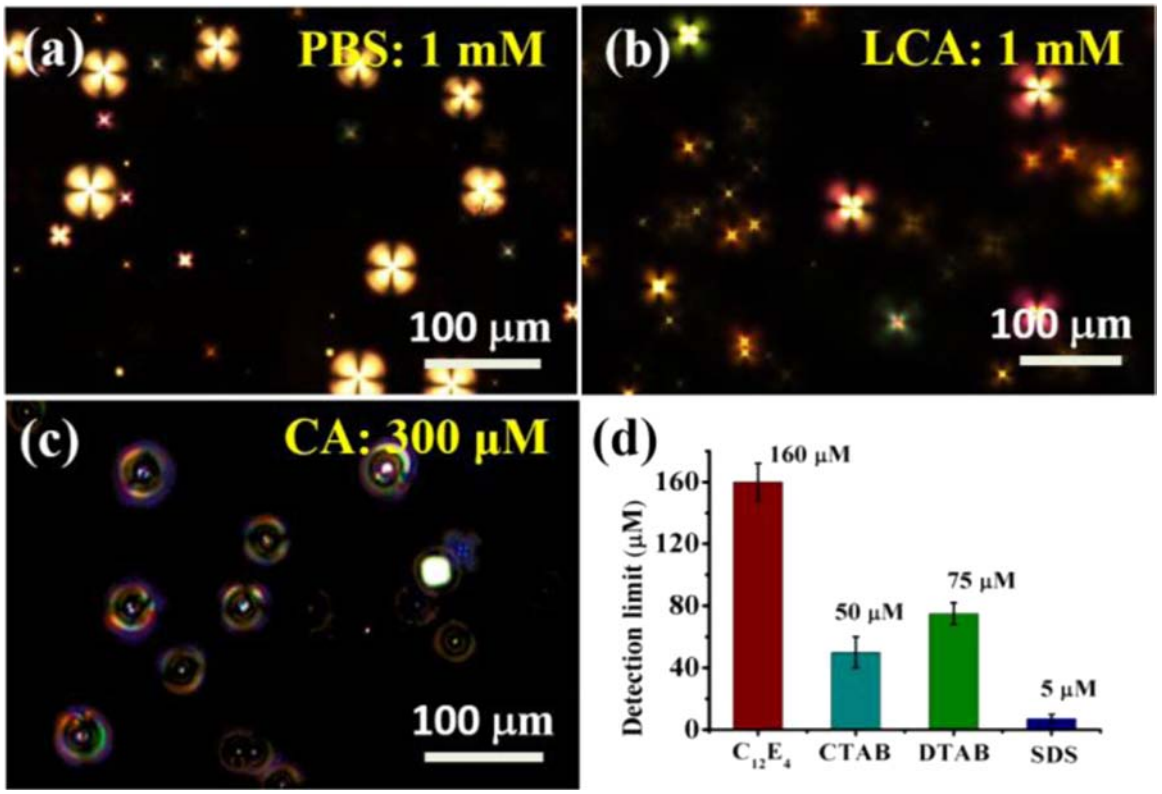

Fig. 7. Optical images of 5CB droplets response to different solutions of (a) 1 mM PBS, (b) 1 mM LCA, and (c) 300 μM CA. (d) Detection limit of CA for different surfactants ($C_{12}E_4$, CTAB, DTAB, SDS). Scale bar: 100 μm.

bromide (DTAB), and SDS were 160 μM, 50 μM, 75 μM, and 5 μM respectively. This result indicates that the SDS has a quite low detection limit. The reason is that $C_{12}E_4$, CTAB and DTAB are more active than SDS, thus the surface of 5CB configuration is difficult to be disrupted in $C_{12}E_4$, CTAB and DTAB by CA, comparing to SDS.

Please cite this article as: X. Niu, et al., Optics Communications (2016), http://dx.doi.org/10.1016/j.optcom.2016.07.016

Table 1
Comparison of performance and properties of this LC sensor with that of previous reports.

No.	Method	Detection limit (μmol/L)	Ref.
1.	Gas chromatography	224	[8]
2.	Nanosensor based on molecular imprinting	38.3	[11]
3	Homeotropic anchoring LC layer sensor	12	[26]
4.	Dispersive LC droplets sensor in surfactant	5	This work

3.5. Comparison of different biosensors for detection of CA

In addition, the comparison of performance and properties of our LC sensor with previous reported methods was given in Table 1. From Table 1, we can see that the detection limit of our LC sensor is much lower than that of previous reports.

4. Conclusions

In this work, a low-cost, simple and fast strategy for sensing of CA based on 4-cyano-4′-penthlbiphenyl (5CB) liquid crystal droplets in phosphate buffer saline (PBS) solution has been developed. The relationship of LC droplets size and stirring time was studied, and the pH value of SDS solution was optimized. A radial-to-bipolar transition of 5CB droplet was triggered during competitive reaction of CA at the SDS surfactant-laden 5CB droplet surface, where the polarization optical images were analyzed to estimate the amount of CA added. Comparing to the CA sensor using liquid crystal film with detection limit of 12 μM, our method has a detection limit of ~5 μM in similar condition, which is also reduces about 58.3%.

Acknowledgments

This work is supported by National Natural Science Foundation of China (NSFC) (61405088 and 11574130), Basic Research of Shenzhen Science and Technology Innovation Council (JCYJ20150601155130435 and JCYJ20150930160634263).

References

[1] J. Han, Y. Liu, R. Wang, J. Yang, V. Ling, C.H. Borchers, Metabolic profiling of bile acids in human and mouse blood by LC-Ms/Ms in combination with phospholipid-depletion solid-phase extraction, Anal. Chem. 87 (2015) 1127–1136.
[2] F.G. Schaap, M. Trauner, P.L.M. Jansen, Bile acid receptors as targets for drug development, Nat. Rev. Gastroenterol. Hepatol. 11 (2014) 55–67.
[3] V. Tremaroli, F. Bäckhed, Functional interactions between the gut microbiota and host metabolism, Nature 489 (2012) 242–249.
[4] X. Zeng, W. Tao, L. Mei, L. Huang, C. Tan, S.-S. Feng, Cholic acid-functionalized nanoparticles of star-shaped PLGA-vitamin E TPGS copolymer for docetaxel delivery to cervical cancer, Biomaterials 34 (2013) 6058–6067.
[5] E. Halilbasic, T. Claudel, M. Trauner, Bile acid transporters and regulatory nuclear receptors in the liver and beyond, J. Hepatol. 58 (2013) 155–168.
[6] M. Tolonen, S. Sarna, M. Halme, Anti-oxidant supplementation decreases TBA reactants in serum of elderly, Biol. Trace Elem. Res. 17 (1988) 221–228.
[7] S. Gu, B. Cao, R. Sun, Y. Tang, J.L. Paletta, X.L. Wu, L. Liu, W. Zha, C. Zhao, Y. Li, J. M. Radlon, P.B. Hylemon, H. Zhou, J. Aa, G. Wang, A metabolomic and pharmacokinetic study on the mechanism underlying the lipid-lowering effect of orally administered berberine, Mol. Biosyst. 11 (2015) 463–474.
[8] T. Ghaffarzadegan, M. Nyman, J.Å. Jönsson, M. Sandahl, Determination of bile acids by hollow fibre liquid-phase microextraction coupled with gas chromatography, J. Chromatogr. B 944 (2014) 69–74.
[9] K. Taguchi, E. Fukusaki, T. Bamba, Simultaneous and rapid analysis of bile acids including conjugates by supercritical fluid chromatography coupled to tandem mass spectrometry, J. Chromatogr. A 1299 (2013) 103–109.
[10] D. Esteban-Gomez, L. Fabbrizzi, M. Licchelli, D. Sacchi, A two-channel chemosensor for the optical detection of carboxylic acids, including cholic acid, J. Mater. Chem. A 15 (2005) 2670–2675.
[11] A. Gültekin, A. Ersöz, A. Denizli, R. Say, Preparation of new molecularly imprinted nanosensor for cholic acid determination, Sens. Actuators B: Chem. 162 (2012) 153–158.
[12] M.J. Paiva, H.C. Menezes, J.C. Cardoso da Silva, R.R. Resende, Z.D.L. Cardeal, New method for the determination of bile acids in human plasma by liquid-phase microextraction using liquid chromatography-ion-trap-time-of-flight mass spectrometry, J. Chromatogr. A 1388 (2015) 102–109.
[13] M.H. Sarafian, M.R. Lewis, A. Pechlivanis, S. Ralphs, M.J.W. McPhail, V.C. Patel, M.E. Dumas, E. Holmes, J.K. Nicholson, Bile acid profiling and quantification in biofluids using ultra-performance liquid chromatography tandem mass spectrometry, Anal. Chem. 87 (2015) 9662–9670.
[14] J.J. Birk, M. Dippold, G.L.B. Wiesenberg, B. Glaser, Combined quantification of faecal sterols, stanols, stanones and bile acids in soils and terrestrial sediments by gas chromatography-mass spectrometry, J. Chromatogr. A 1242 (2012) 1–10.
[15] S. Jäntti, M. Kivilompolo, L. Öhrnberg, K. Pietiläinen, H. Nygren, M. Orešič, T. Hyötyläinen, Quantitative profiling of bile acids in blood, adipose tissue, intestine, and gall bladder samples using ultra high performance liquid chromatography-tandem mass spectrometry, Anal. Bioanal. Chem. 406 (2014) 7799–7815.
[16] S. Herminghaus, K. Jacobs, K. Mecke, Spinodal dewetting in liquid crystal and liquid metal films, Science 282 (1998) 916–919.
[17] S.J. Woltman, G.D. Jay, G.P. Crawford, Liquid crystal materials find a new order in biomedical applications, Nat. Mater. 6 (2007) 929–938.
[18] S.E. Moulton, M. Maugey, P. Poulin, G.G. Wallace, Liquid crystal behavior of single-walled carbon nanotubes dispersed in biological hyaluronic acid solutions, J. Am. Chem. Soc. 129 (2007) 9452–9457.
[19] J. Fan, Y.N. Li, H.K. Bisoyi, R.S. Zola, D.K. Yang, T.J. Bunning, D.A. Weitz, Q. Li, Light-directing omnidirectional circularly polarized reflection from liquid crystal droplets, Angew. Chem. Int. Ed. 54 (2015) 2164–2188.
[20] B.D. Hamlington, B. Steinhaus, J.J. Feng, Liquid crystal droplet production in a microfluidic device, Liq. Cryst. 34 (2007) 861–870.
[21] S. Sivakumar, K.L. Wark, J.K. Gupta, N.L. Abbott, F. Caruso, Liquid crystal emulsions as the basis of biological sensors for the optical detection of bacteria and viruses, Adv. Funct. Mater. 19 (2009) 2260–2265.
[22] V.J. Aliño, J. Pang, K.L. Yang, Liquid crystal droplets as a hosting and sensing platform for developing immunoassays, Langmuir 27 (2011) 11784–11789.
[23] U. Manna, Y.M. Zayas Gonzalez, R.J. Carlton, F. Caruso, N.L. Abbott, D.M. Lynn, Liquid crystal chemical sensors that cells can wear, Angew. Chem. Int. Ed. 52 (2013) 14011–14015.
[24] S.H. Yoon, K.C. Gupta, J.S. Borah, S.Y. Park, Y.K. Kim, J.H. Lee, I.K. Kang, Folate ligand anchored liquid crystal microdroplets emulsion for in vitro detection of KB cancer cells, Langmuir 30 (2014) 10668–10677.
[25] F. Merola, S. Grilli, S. Coppola, V. Vespini, S.D. Nicola, P. Maddalena, Reversible fragmentation and self-assembling of nematic liquid crystal droplets on functionalized pyroelectric substrates, Adv. Funct. Mater. 22 (2012) 3267–3272.
[26] Q.Z. Hu, C.H. Jang, Spontaneous formation of micrometer-scale liquid crystal droplet patterns on solid surfaces and their sensing applications, Soft Matter 9 (2013) 5779–5784.
[27] S. He, W. Liang, C. Tanner, K.L. Cheng, J. Fang, S.T. Wu, Liquid crystal based sensors for the detection of cholic acid, Anal. Methods 5 (2013) 4126–4130.
[28] S.C. Oscar, M.V. Yamir, J.L.G. Juan, J.C. Antoranz, Criticality in droplet fragmentation, Phys. Rev. Lett. 76 (1996) 42–45.

Please cite this article as: X. Niu, et al., Optics Communications (2016), http://dx.doi.org/10.1016/j.optcom.2016.07.016